



## Design and Simulation of a Bidirectional Isolated DC–DC Converter for a Battery Energy Storage System

Patel Nilay Anilbhai Tandel Jay S.  
Electrical Engineering.MGITER Navsari,  
Electrical Engineering.MGITER Navsari

*Abstract-Photovoltaic(PV) system have been installed in some residential house, schools and buildings without energy storage systems. Massive penetration of PV systems with the capability of exporting electric power into the grid, but without energy storage systems can affect the grid due to their intermittent nature. Therefore, integration of energy storage systems is essential to make the output power of PV systems dispatchable in supply and demand control. High-efficiency power converters are indispensable to charging and discharging of energy storage devices. The main goals of the project included the implementation of two modes of operation: a battery discharge mode where current is being fed into the grid and a battery charging mode in which current is pulled from the grid and put into the batteries. A secondary goal of the design was to ensure that the current being injected into grid was at or near unity power factor. The three-phase, full-bridge bidirectional isolated dc–dc converter was introduced for high power-density power conversion systems. This converter works as the interface between the battery pack and the ac grid, which needs to meet the requirements of bidirectional power flow capability and to ensure high power factor and low THD as well as to regulate the dc side power regulation. All simulation of energy storage system, bidirectional dc-dc converter and high frequency transformer are obtained from MATLAB Simulink Environment.*

*key words-* Bidirectional isolated dc–dc converters, dc-bias currents, energy storage systems, lithium-ion (Li-ion) battery.

### I.INTRODUCTION

Bidirectional dc-dc converters (BDC) have recently received a lot of attention due to the increasing need to systems with the capability of bidirectional energy transfer between two dc buses. Apart from traditional application in dc motor drives, new applications of BDC include energy storage in renewable system.

The fluctuation nature of most renewable energy resources, like wind and solar, makes them unsuitable for standalone operation as the sole source of power. A common solution to overcome this problem is to use an energy storage device besides the renewable energy resource to compensate for these fluctuations and maintain a smooth and continuous power flow to the load. As the most common and economical energy storage devices in medium-power range are batteries and super-capacitors, a dc-dc converter is always required to allow energy exchange between storage device and the rest of system. Such a converter must have bidirectional power flow capability with flexible control in all operating modes.

In HEV applications, BDCs are required to link different dc voltage buses and transfer energy between them. For example, a BDC is used to exchange energy between main batteries (200-300V) and the drive motor with 500V dc link. High efficiency, lightweight, compact size and high reliability are some important requirements for the BDC used in such an application. BDCs also have applications in line-interactive UPS which do not use double conversion technology and thus can achieve higher efficiency. In a line-interactive UPS, the UPS output terminals are connected to the grid and therefore energy can be fed back to the inverter dc bus and charge the batteries via a BDC during normal mode. In backup mode, the battery feeds the inverter dc bus again via BDC but in reverse power flow direction.

Lithium-ion based battery energy storage system has become one of the most popular forms of energy storage system for its high charge and discharge efficiency and high energy density. This dissertation proposes a high-efficiency grid-tie lithium-ion battery based energy storage system, which consists of a LiFePO<sub>4</sub> battery based energy storage and associated battery management system (BMS), a high-efficiency bidirectional dc-dc converter and the central control unit which controls the operation mode and grid interface of the energy storage system. The BMS estimates the state of charge and state of health of each battery cell in the pack and applies active charge equalization to balance the charge of all the cells in the pack. The bidirectional dc-dc converter works as the interface between the battery pack and the ac grid, which needs to meet the requirements of bidirectional power flow capability and to ensure high power factor and low THD as well as to regulate the dc side power regulation.

The bidirectional dc-dc converter along with energy storage has become a promising option for many power related systems, including hybrid vehicle, fuel cell vehicle, renewable energy system and so forth. It not only reduces the cost and improves efficiency, but also improves the performance of the system.

The design project was focused on building a scaled down battery energy storage system. The design was required to utilize power electronics to interface a battery bank with the grid. The system was required to operate in two modes, the “discharge mode” in which power is drawn from the batteries and injected into the grid. The design was also required to recharge the battery bank from the grid during a “charge mode” of operation. High frequency step down transformer used to charging and discharging battery at nominal level voltages.

## II CIRCUIT DIAGRAM

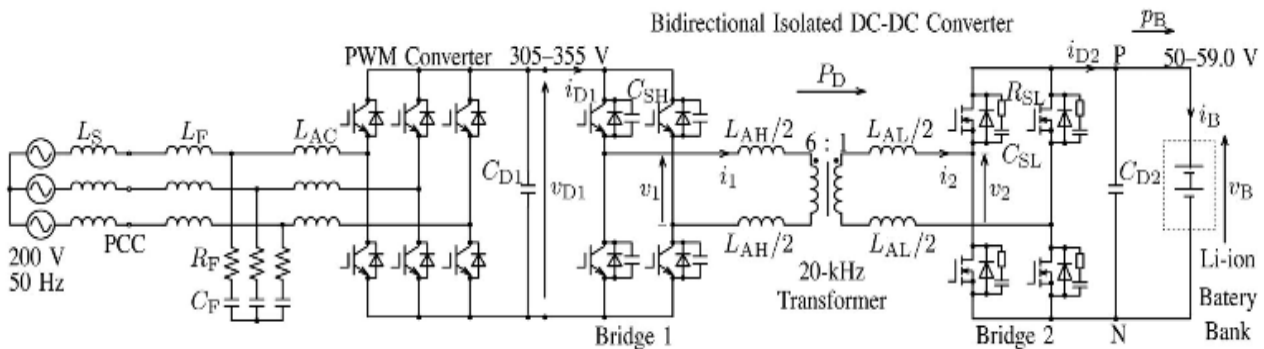


**Figure 1.1** Li-ion battery bank of 53.2 V, 40 A·h connected to the 6-kW bidirectional isolated dc-dc converter, where  $L_S$  is the background system impedance ( $<1\%$ ),  $L_{AC} = 280\mu H$  (1.3%),  $L_F = 44\mu H$  (0.2%),  $R_F = 0.2\Omega$  (3%), and  $C_F = 150\mu F$  (33%) on a three-phase 200-V, 6-kW, and 50-Hz base.

The transformer used in an isolated dc dc converter can experience magnetic flux saturation due to a dc-bias current flowing in it. As a result, high-current pulses can be observed in the ac current. They cause additional current stress in the switching devices, reduce efficiency, and may damage the dc-dc converter in the worst case. The so-called “dc blocking capacitors” are typically used to prevent the transformer from magnetic- flux saturation. However, available high frequency capacitors may not meet high current requirements. Parallel connections of multiple capacitors are accompanied by bulkiness, increased cost, and decreased reliability. Krismer and Kolar designed a 100-kHz transformer with a low magnetic-flux density not only to achieve a low core loss but also to provide a large safety margin prior to the saturation flux density. However, they did not address any dc-bias current in the transformer. Klopper and Ferreira proposed a sensor for measurement of flux below a saturation level.

This paper presents the 53.2-V, 2-kW·h Li-ion battery energy storage system based on the 6-kW full-bridge bidirectional isolated dc–dc converter using a 20-kHz transformer. However, this paper aims at demonstrating the performance of the bidirectional isolated dc–dc converter for low-voltage and high-current battery applications. It provides experimental and theoretical discussions concerning the effect of dc-bias currents on the magnetic-flux saturation of the high-frequency transformer. This consideration helps in designing an appropriate air-gap length in high-frequency transformers with different voltage and current ratings. The overall loss breakdown of the dc–dc converter compares the loss distribution of the low-voltage high-current converter with that of the high-voltage low-current converter.

### III SYSTEM CONFIGURATION

Fig 1.2 shows the experimental setup consisting of a three-phase pulse-width modulated (PWM) converter, the 6-kW bidirectional isolated dc–dc converter, and the 53.2-V, 40-A·h Li-ion battery bank. The PWM converter is connected at the point of common coupling to the 200-V, 50-Hz ac-side through the ac-link inductor  $L_{ac}$ , and the switching-ripple-filter circuit is represented by  $L_F$ ,  $C_F$ , and  $R_F$ . The battery bank consists of two 26.6-V, 40-A·h Li-ion battery modules connected in series. Note that both the nominal battery voltage of 53.2 V and the operating voltage range of are determined from a practical point of view, considering system-level safety, cost, and reliability. The high-voltage dc bus is adjusted to keep the dc-voltage ratio of the HVS to LVS close to the transformer turns ratio. The dc–dc converter with a symmetrical structure consists of two voltage- source converters that are referred to as bridge 1 and bridge 2 in this paper. To minimize stray inductances, the LVS uses laminated bus bars so that ripple currents can flow into the dc capacitor CD2 that is the combination of electrolytic capacitors and high-frequency film capacitors.

Bridge 1 consists of four 600-V, 200-A trench-gate IGBTs. Each IGBT module contains two devices in series. A lossless capacitor is connected in parallel with each of the IGBTs to achieve zero voltage switching and to minimize turn off overvoltage across the collector–emitter terminals of the IGBT.

Model Name	LIM40-7D1-S1
Capacity	40 Ah
Nominal Voltage	26.6 V (= 3.8 V × 7)
Rated Rapid Charging Current	120 A (3C)
Rated Discharge Current	200 A (5C)
Operating Temperature	0–45 °C
Weight	17 kg

Courtesy of GS Yuasa [19].



Figure 1.2 Photo of the two Li-ion battery modules used for experiment, each of which is rated at 26.6 V and 40 A·h

Bridge 2 consists of four 100-V, 500-A MOSFETs (PDM5001). Each MOSFET module also contains two devices in series. From the datasheet by Nihon Inter Electronics Corporation, the on-state resistance,  $R_{DS(ON)}$ , is as low as 0.5 m $\Omega$ .

However, the sum of the wire bond resistance, contact resistance between the source and drain metallization and the silicon, and the contact resistance between the metallization and lead frame is not negligible because the total resistance  $R_{wcm1}$  reaches 0.6 m $\Omega$ .

Bridge 2 is operated in synchronous rectification mode to minimize conduction loss. A small-sized RC snubber is connected in parallel, with each of the four MOSFETs, to reduce its switching loss and to damp out an overvoltage and the resultant ringings.

Figure presents the specifications of the Li-ion battery modules of the Li-ion battery bank shown in Fig. 1. Each of the modules consists of seven Li-ion battery cells connected in series, where the nominal voltage of each battery cell is 3.8 V. From the specifications given, the specific energy of the Li-ion battery module can be determined to be 63 W·h/kg, and its specific power to be 313 W/kg. Fig. shows the photo of the two Li-ion battery modules used in the experimental setup. No voltage balancing circuit is required for the series-connected battery modules.

#### IV CONTROL METHOD

The control method is based on an open-loop, feed forward control intended for investigating the basic operating performance of the dc–dc converter in the Li-ion battery energy storage system. Altera's Max 7000s complex programmable logic device is used to generate eight gate signals for all the gate-drive circuits of the IGBTs in bridge 1 and the MOSFETs in bridge 2. The switching periods of bridges 1 and 2 are the same as 50  $\mu$ s (20 kHz). Due to the existence of finite turn on and turn off times of the IGBTs and MOSFETs, a dead time of 1.24  $\mu$ s is set for each leg in bridges 1 and 2. The time resolution of the controller is 40 ns/bit, i.e., 0.29°/bit.

ADJUSTMENT OF HVS DC-LINK VOLTAGE WITH BATTERY VOLTAGE

Charging		Discharging	
$v_B$ [V]	$v_{D1}$ [V]	$v_B$ [V]	$v_{D1}$ [V]
54.7–55.5	330	55.9–55.2	340
55.9–57.6	340	55.3–54.2	330
58.0–58.4	345	53.9–53.1	320
58.5–59.0	355	53.1–52.1	315
–	–	51.7–50.0	305

Table 1. 1 DJUSTMENT OF HVS DC-LINK VOLTAGE WITH BATTERY VOLTAGE

Table 1.1 indicates the relation between the dc voltage at the HVS,  $v_{D1}$  and the battery voltage  $v_B$  during battery charging and discharging. The battery charging operation is carried out from an initial voltage of 54.7 V, and the discharging operation is carried out from an initial voltage of 55.9 V. The initial voltage is measured at  $i_B=0$ . The dc voltage  $v_{D1}$  is controlled with the battery voltage  $v_B$  in such a way as to minimize the voltage change across the auxiliary inductors and transformer leakage inductor. Adjustment of  $v_{D1}$  is carried out by changing the reference voltage of the three-phase PWM converter.

#### V CONVERTER EFFICIENCY

Fig. 1.3 shows the measured plots of the dc–dc converter efficiency and the battery terminal voltage when the battery is charged and discharged between 500 W and 5.9 kW. Power at the HVS,  $P_{dc1}$  is calculated from measurements of  $v_{D1}$  and  $i_{D1}$ , and the battery power  $P_B$  is calculated from measurements of  $v_B$  and  $i_B$  by using the Hioki 3139 power meter having a moving average function. The losses in the Li-ion battery, the PWM converter, and the cables connecting the battery and PWM converter to the dc–dc converter are not considered. Therefore, this paper will consider the low-side dc-link voltage as the battery voltage  $v_B$ .

The accuracies of the measuring instruments are listed in the Appendix. The measured efficiency points in Fig. 1.3 are fitted with an exponential function, whereas the measured battery voltage points are fitted with a first-order polynomial function. Note that both functions use the least-mean-square approximation.

The efficiency of the dc-dc converter is less than 92% at low power levels (<1 kW). As bridge 2 is operated in synchronous rectification, the conduction loss in bridge 2 should not be significant at a low conduction current. The conduction loss in bridge 1, the snubber loss due to hard switching or incomplete zero-voltage switching, and the switching loss in bridges 1 and 2 would dominate the loss at this low-power level. At battery charging, the measured converter efficiency peaks at 96% at  $P_B=1.6\text{ kW}$ . At battery discharging, measured converter efficiency averages at 96.8% between  $P_B=-1.2\text{ kW}$  and  $P_B=-2.2\text{ kW}$ . The maximum efficiency of the converter is achieved around the onset of zero-voltage switching. An observable decrease in converter efficiency exists when the battery power is between  $\pm 3$  and  $\pm 6$  kW. This is the result from an increase in conduction, copper, ohmic, and switching losses, as the operating current increases to 100 A during battery charging, and to 120 A during battery discharging at the LVS. The estimation of loss breakdown is shown in Section V.

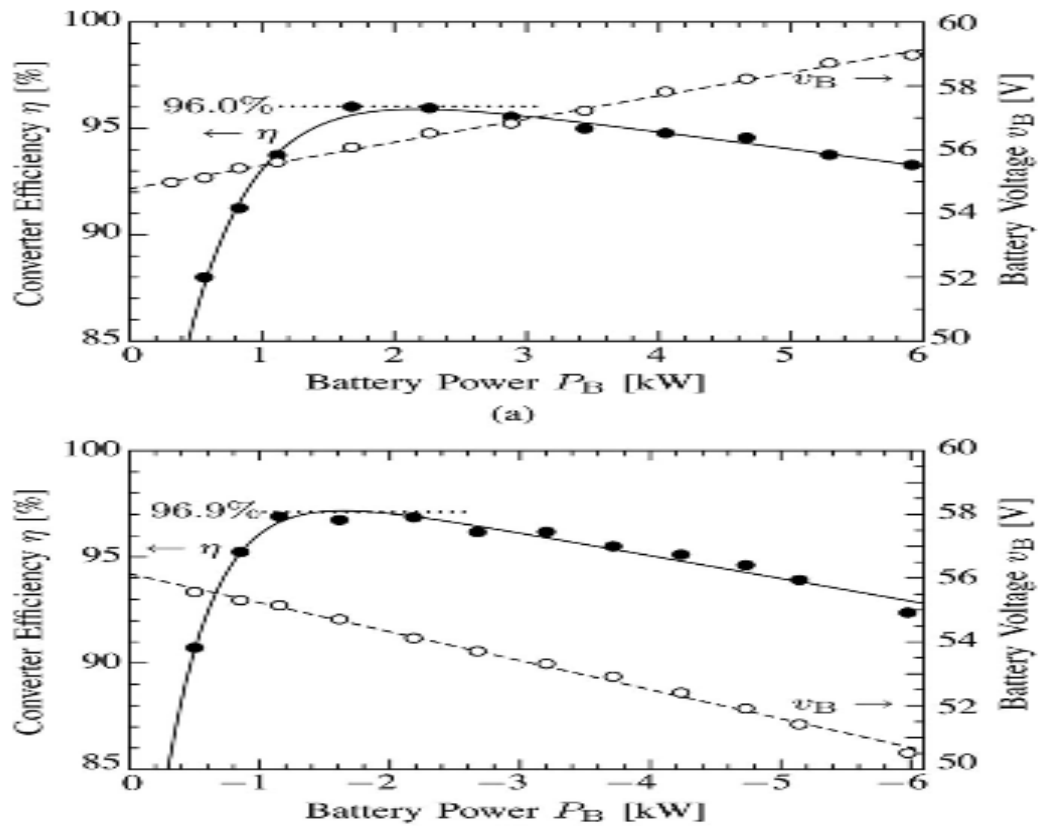


Figure 1. 3 Measured dc-dc converter efficiencies and battery voltages for Battery Charging and Battery discharging.

## VI SIMULATION AND RESULT

Simulation Model of Bidirectional DC-DC Converter For Power Flow in forward direction are given below.

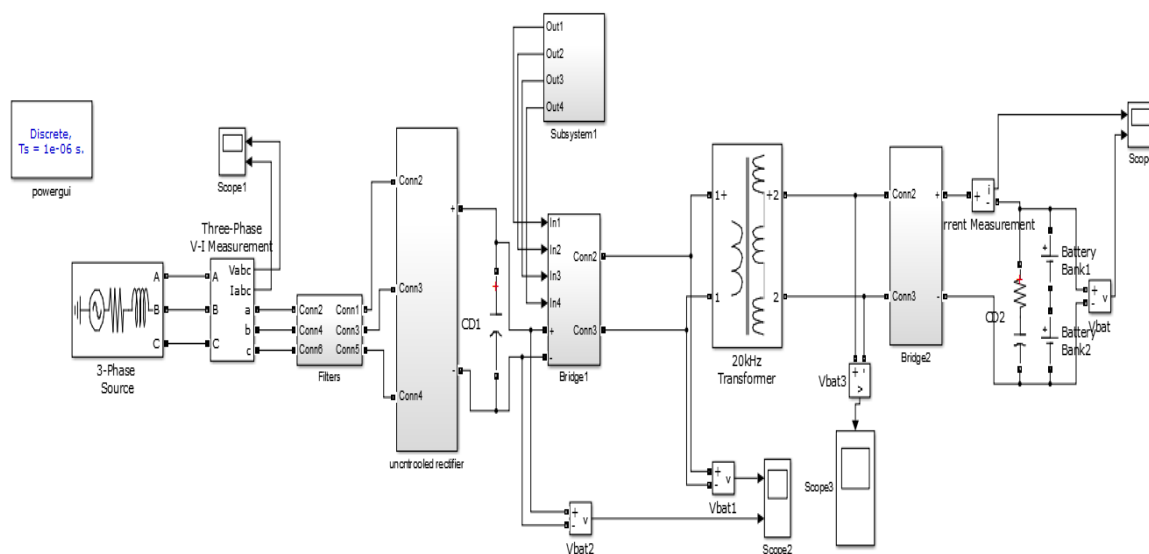


Figure 1. 4 Simulation Model of Bidirectional DC-DC Converter For Power Flow in forward direction

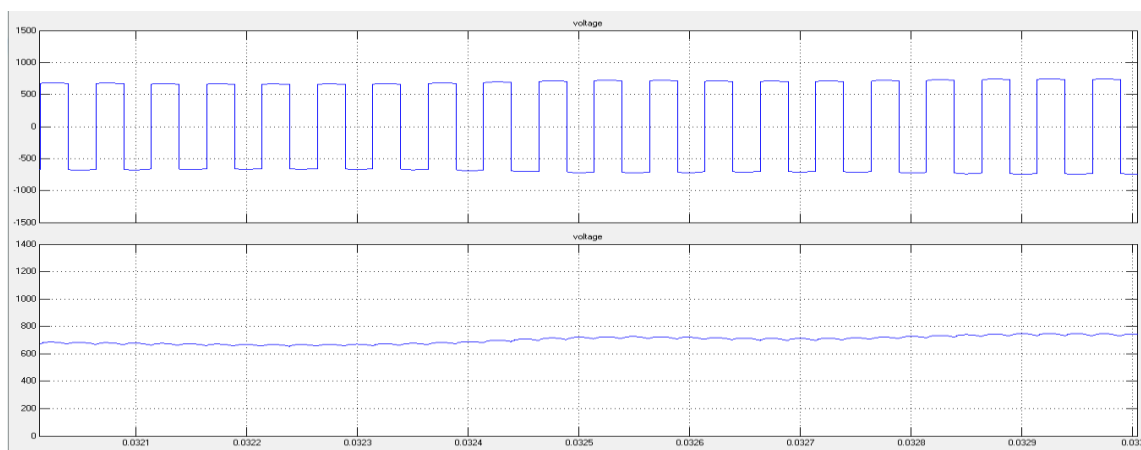


Figure 1. 5 Voltages at HVS of transformer and bridge 1

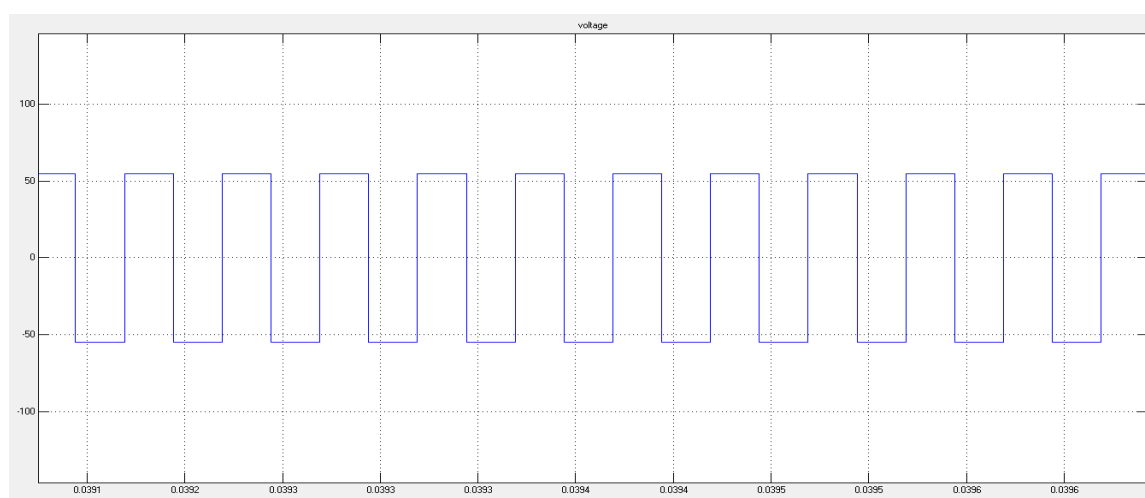


Figure 1. 6 Voltages at LVS of Transformer



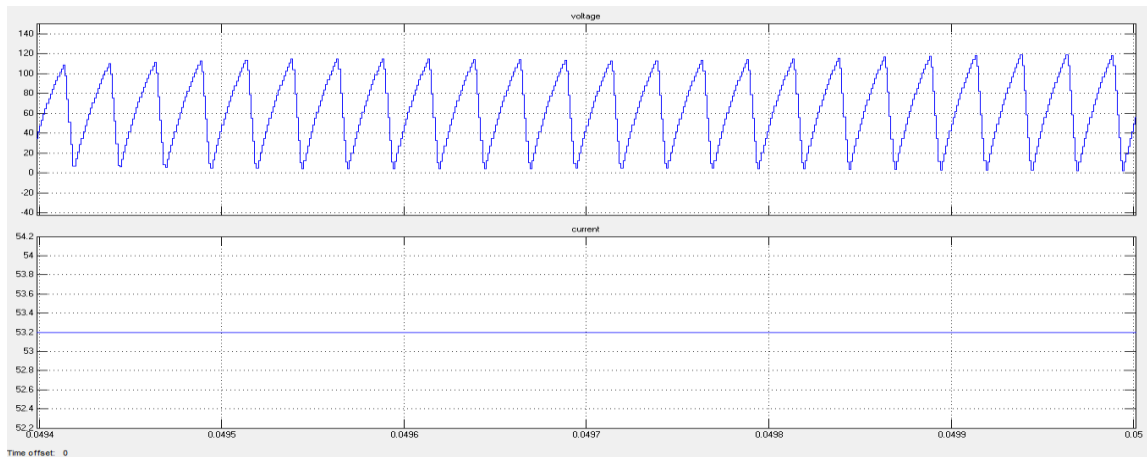


Figure 1. 7 Voltages and Current of lithium-ion battery bank

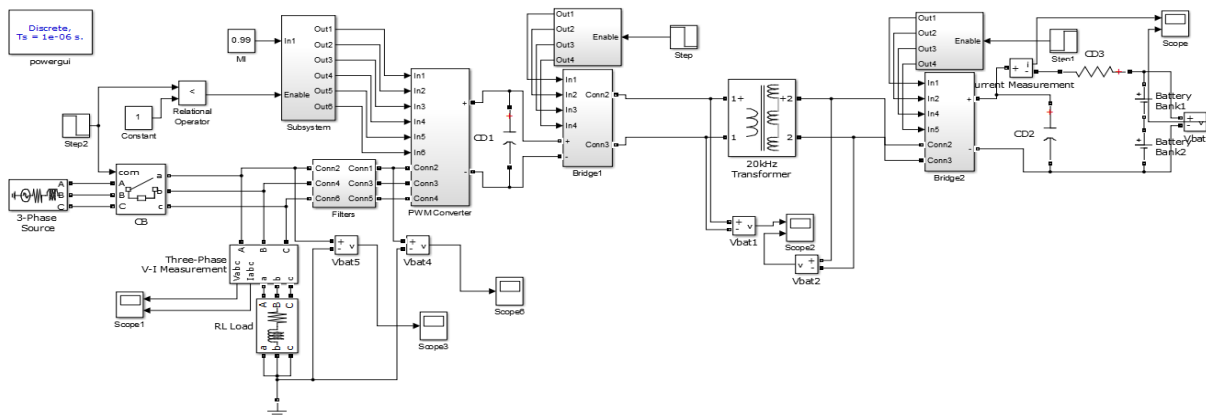


Figure 1. 8 Simulation Model of Bidirectional DC-DC Converter For Power Flow in both direction

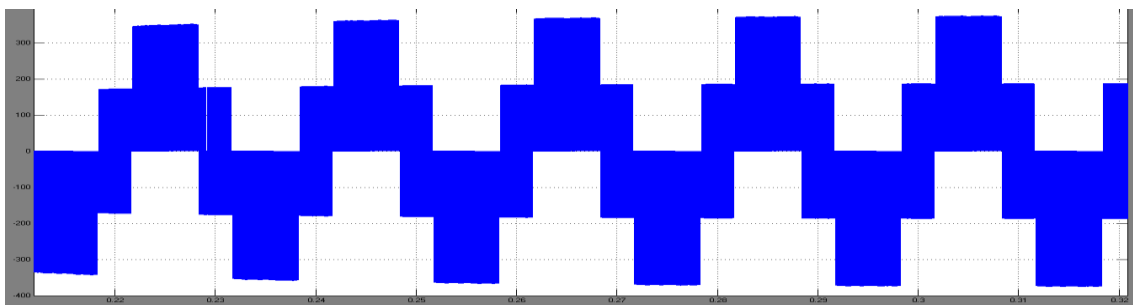


Figure 1. 9 Reverse Voltage without filtering

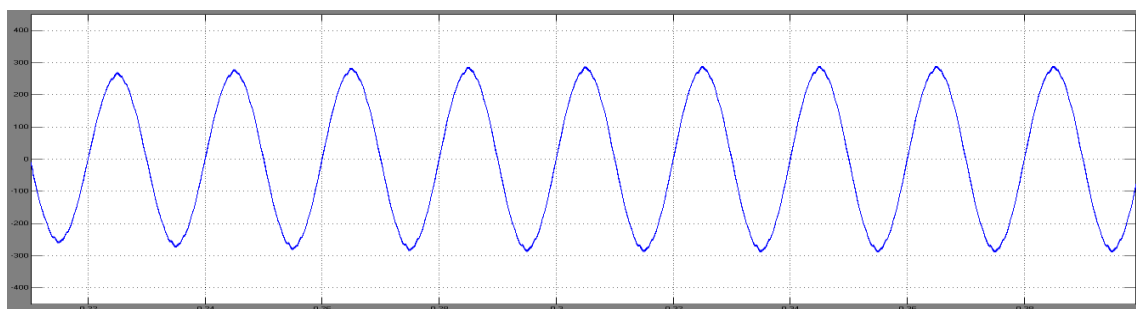


Figure 1. 10 Filtered Reverse Voltage

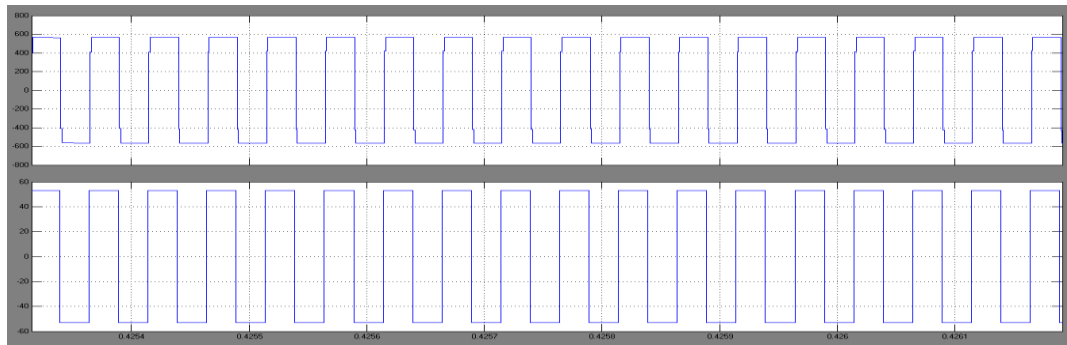


Figure 1. 11 Reverse direction voltages of Transformer at both primary and secondary side

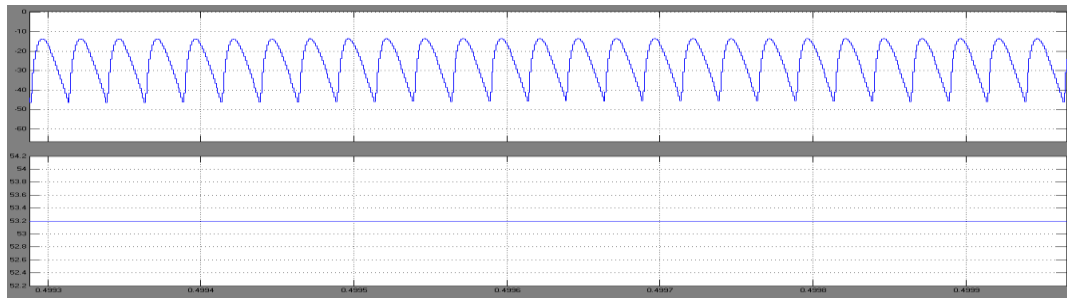


Figure 1. 12 Reverse Current and voltage at battery bank

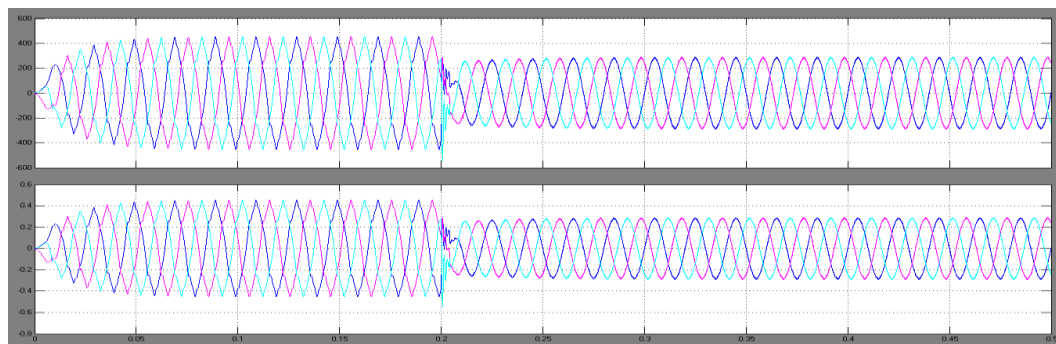


Figure 1. 13 Forward and Reverse voltages at 3 phase load side

## VII CONCLUSION

This paper has presented the experimental results from the combination of a 53.2-V, 40A·h Li-ion battery bank with a single-phase full-bridge bidirectional isolated dc–dc converter. The results have verified the proper operation of the Li-ion battery energy storage system. Discussions focusing on magnetic-flux saturation due to unavoidable dc-bias currents at the high-voltage and LVSs have been carried out. The transformer with an air-gap length of 1 mm has been shown experimentally to be robust against magnetic-flux saturation, even in the worst cases. The bidirectional isolated dc–dc converter exhibits high efficiency in the low-voltage and high-current operation. From the estimation of loss distribution in the dc–dc converter, a large portion of the loss at the rated power is caused by the turn off switching loss at the LVS. One of the best methods of improving the efficiency of the dc–dc converter is to operate it at a lower switching frequency. However, this method is accompanied by acoustic noise generation and a bulky transformer.



## VIII REFERENCES

- 1) Nadia Mei Lin Tan, Takahiro Abe, and Hirofumi Akagi "Design and Performance of a Bidirectional Isolated DC-DC Converter for a Battery Energy Storage System".
- 2) Bidirectional DC-DC Power Converter Design Optimization, Modeling and Control by Junhong Zhang
- 3) P. F. Ribeiro, B. K. Johnson, M. L. Crow, A. Arsoy, and Y. Liu, "Energy storage systems for advanced power applications," Proc. IEEE, vol. 89, no. 12, pp. 1744–1756, Dec. 2001.
- 4) Analysis and Design of Controller for PWM Rectifiers S.Arivarasan M.E Scholar, Division of Power Electronics & Drives, DEEE, CEG Anna University, Chennai, Tamilnadu, India
- 5) Application of Sinusoidal Pulse Width Modulation Based Matrix Converter as Revolutionized Power Electronic Converter K. Vijayakumar, R. Sundar Raj and S. Kannan
- 6) Modeling and Optimization of Bidirectional Dual Active Bridge DC-DC Converter Topologies A dissertation submitted to ETH ZURICH
- 7) Design and Implementation of carrier based Sinusoidal PWM Inverter Pankaj H Zope, Pravin G.Bhangale, Prashant Sonare, S.R.Suralkar
- 8) L. Zhu, "A novel soft-commutating isolated boost full-bridge ZVS-PWM dc-dc converter for bidirectional high power applications," IEEE Trans. Power Electron., vol. 21, no. 2, pp. 422–429, Mar. 2006
- 9) H. Tao, A. Kotsopoulos, J. L. Duarte, and M. A. M. Hendrix, "Transformer-coupled multiport ZVS bidirectional dc-dc converter with wide input range," IEEE Trans. Power Electron., vol. 23, no. 2, pp. 771–781, Mar. 2008. Grid Energy Storage" U.S. Department of Energy December 2013
- 10) D. Vinnikov, J. Laugis, and I Galkin, "Middle-frequency isolation transformer design issues for the high-voltage dc-dc converter," in Proc. IEEE Power Electron. Spec. Conf. (PESC), Jun. 2008, pp. 1930–1936.
- 11) "Electrical Energy Storage" International Electrotechnical Commission 3 rue de Varembe PO Box 131 CH-1211 Geneva 20 Switzerland
- 12) Y. Xie, J. Sun, and S. Freudenberg, "Power flow characterization of a bidirectional galvanically isolated high-power dc/dc converter over a wide operating range," IEEE Trans. Power Electron. vol. 25, no. 1, pp. 54–66, Jan. 2010.
- 13) Hamid R. Karshenas, Hamid Daneshpajoo, Alireza Safaee Praveen Jain and Alireza Bakhshai "Bidirectional DC-DC Converters for Energy Storage Systems". A.M. Gole, 2000 24.437 Power Electronics "Sinusoidal Pulse width modulation".
- 14) Sanjay N. Patel, Jay A. Purohit, Jay D. Panchal "Newest Electrical Energy Storage System: SMES, SCES and BESS".
- 15) S. Begag, N. Belhaouchet and L. Rahmani "Three-Phase PWM Rectifier with Constant Switching Frequency".
- 16) Dr.K.Ravichandrudu, Sk.Fathima, Mr.P.Yohan Babu, Mr.G.V.P.Anjaneyulu "Design and Performance of a Bidirectional Isolated Dc-Dc Converter for Renewable Power System".
- 17) Bi-Directional Inverter and Energy Storage System Submitted to fulfill the requirements of: Texas Instruments Analog Design Contest by Derik Trowler and Bret Whitaker May 2008 University of Arkansas
- 18) M. Jain, M. Daniele, P. K. Jain, "A bidirectional dc-dc converter topology for low power application," IEEE Trans. Power Electron., vol. 15, no. 4, pp. 595–606, 2000